# Changing forms and sudden smooth transitions of tsunami waves

R. H. J. Grimshaw[1], J. C. R. Hunt[1] & K. W. Chow[2],

[1]Department of Mathematics, University College London, UK

[2]Department of Mechanical Engineering, University of Hong Kong, Hong Kong

July 17, 2014

**Abstract**

In some tsunami waves travelling over the ocean, such as the one approaching the eastern coast of Japan in 2011, the sea surface of the ocean is depressed by a small meter-scale displacement over a multi-kilometer horizontal length scale, lying in front of a positive elevation of comparable magnitude and length, which together constitute a down-up or "breather" wave. Shallow water theory shows that the latter travels faster than the former and, according to an extended Korteweg-de Vries model presented here, the waves undergo a transition. Firstly the two parts coincide at a given position and time producing a maximum elevation, whose amplitude depends on the shape of the approaching wave. Typically this amplitude is larger than the initial displacement magnitude by a factor which can be as large as two, which may explain anomalous elevations of tsunamis at particular positions along their trajectories. It is physically significant that for these small amplitude waves, no wave breaking occurs and there is no excess dissipation. Secondly, following the transition, the elevation wave moves ahead of the depression wave and the distance between them increases either linearly or logarithmically with time. The implications for how these "down-up" tsunami waves reach the shoreline are considered.

## 1 Introduction

Tsunamis are generated by submarine earthquakes, and sometimes by landslides or volcanic eruptions. In general the tsunami wave at the source can be either a wave of depression, or of elevation, or a combinations of these, see the recent assessments by Arcasi and Segur (2012) and Dias *et al* (2014). As the wave propagates shorewards over the continental slope and shelf, and finally impacting the shoreline, the increasing effect of nonlinearity will lead to quite different set of behaviours depending on the wave polarity, see Carrier *et al* (2003) and Fernando *et al* (2008) for instance. Although the depression waves can cause as much or more damage than elevation waves, they have not been studied as much as elevation waves. However, their potential importance has been noted in the theoretical studies by Tadepalli and Synolakis (1994, 1996), in the analysis of field data by Soloviev and Mazova (1994) and in the experiments of Kobayashi and Lawrence (2004), Klettner *et al* (2012), Rossetto *et al* (2011) and Charvet *et al* (2013).

Most studies of the connection between the incident wave shape and polarity, and the consequent shoreline impact, have used the linear and nonlinear shallow water equations, see Tadepalli and Synolakis (1994, 1996), Carrier *et al* (2003), Madsen and Schaffer (2010) and Didenkulova and Pelinovsky (2011) for instance. However, although these models have proved valuable and insightful, they are non-dispersive and hence do not capture the effects of wavenumber dispersion as the tsunami waves develop shorter length scales in their propagation shoreward. In particular when shocks, or $N$-waves, are predicted by these models, the discontinuity needs to be resolved either with some turbulent wave-breaking model, or by the inclusion of some wave dispersion. The latter choice is the focus of this paper, where our aim is to exhibit some exact solutions of certain model equations, whose range of dynamical behaviour is potentially interesting in the context of tsunamis when these involve depression waves, and interactions between depression and elevation waves.

The combination of weak nonlinearity and weak linear dispersion leads typically to a Korteweg-de Vries (KdV) equation, or to a Bousinesq system, see Segur (2007) and related articles in the compilation by Kundu (2007) for the tsunami context. However, much of the tsunami literature has focussed on the classical solitary wave solution, which is always a wave of elevation. Hence, in this paper, we use a suite of KdV-type equations to examine how waves of depression evolve. It is pertinent to note here that the critique of the validity of KdV theories by Madsen and Schaffer (2010) and Arcasi and Segur (2012), amongst others, are based on solitary wave dynamics, and we suggest that this may be a rather restrictive view of the value of KdV theories.

In section 2 we re-examine the KdV equation, equation (1) below, both for a constant depth, and for variable depth, with the main aim of demonstrating the structure of depression waves. Then in section 3 we present an extended KdV equation model, expressed in terms of an augmented dependent variable, which contains both quadratic and cubic nonlinearity, with coefficients of the same positive sign. There is then a family of two-soliton and breather solutions, which demonstrate striking interactions between a depression wave and an elevation wave. We are especially concerned with the scenario when the approaching tsunami wave, propagating with a speed $c$ which depends on the depth $h$, and also on the wave amplitude, consists of a depression wave of magnitude $\Delta h \ll h$ and horizontal length scale $L_0 \gg h$, in front of an elevation wave of comparable magnitude, constituting an down-up wave, or isosceles $N$-wave in the terminology of Tadepalli and Synolakis (1994). This configuration was observed in the Sumatra tsunami of 2004, see Ioulalen *et al* (2007) and Grilli *et al* (2007), and that in Tohoku in 2011 see Mori *et al* (2013), and was examined in experiments by Klettner *et al* (2012) motivated in part by these observations. Shallow water theory implies that the elevation will travel faster with a speed difference $\Delta c \sim \sqrt{g\Delta h}$, and then after a time $t^* \sim L_0/\Delta c$ the waves undergo a transition. First, the two parts coincide and produce a maximum elevation $\beta\Delta h$, where based on the afore-mentioned two-soliton and breather solutions, we estimate that

$1 \leq \beta \leq 2$ and $\beta = 2$ when the depression and elevation waves are of equal amplitude magnitudes. Second, the elevation wave then moves ahead of the depression wave and the distance between them increases in proportion to $(t - t^*)$ or $\log(t - t^*)$ for the two-soliton or breather solutions respectively. These estimates may explain anomalous elevations of some tsunamis at particular positions along their trajectories, noting that for these small amplitude waves, there is very little dissipation. We conclude with a discussion in section 4.

# 2 Korteweg-de Vries equation

The Korteweg-de Vries equation on a variable depth is,

$$\zeta_t + c\zeta_x + \frac{c_x}{2}\zeta + \frac{3c}{2h}\zeta\zeta_x + \frac{ch^2}{6}\zeta_{xxx} = 0\,. \tag{1}$$

Here $\zeta(x,t)$ is the free surface elevation above the undisturbed depth $h(x)$, while $c(x) = \sqrt{h(x)}$ is the linear long wave phase speed, using non-dimensional units based a length scale $h_0$ and a time scale $\sqrt{h_0/g}$. Equation (1) was derived for surface gravity waves by Johnson (1973a,b), and an analogous general equation for both surface and internal waves by Grimshaw (1981). The first two terms in (1) are the dominant terms, and by themselves describe the propagation of a linear long wave with speed $c$. The derivation uses the usual KdV balance in which the $\partial/\partial x \sim \epsilon \ll 1$, $A \sim \epsilon^2$, and weak inhomogeneity is added so that $c_x/c$ scales as $\epsilon^3$.

Equation (1) is in the form appropriate for an initial value problem. For application to tsunami waves, it is useful to cast it into a form describing evolution along the wave path. Thus, a form asymptotically equivalent to (1) is

$$\zeta_\tau + \frac{h_\tau}{4h}\zeta + \frac{3}{2h}\zeta\zeta_\xi + \frac{h}{6}\zeta_{\xi\xi\xi} \; = \; 0\,, \tag{2}$$

$$\text{where} \quad \tau = \int_0^x \frac{dx'}{c(x')}, \qquad \xi = \tau - t. \tag{3}$$

Here $\tau$ is a time-like variable measuring travel time along the wave path, and in variable depth, $h = h(\tau)$. This governing equation (2) can be cast into several equivalent forms.

$$\eta = h^{1/4}\zeta\,, \quad \text{so that} \quad \eta_\tau + \frac{3}{2h^{5/4}}\eta\eta_\xi + \frac{h}{6}\eta_{\xi\xi\xi} \; = \; 0\,. \tag{4}$$

This form shows that equation (2) has two integrals of motion with the densities proportional to $\eta = h^{1/4}\zeta$ and $\eta^2 = h^{1/2}\zeta^2$. These are often referred to as laws for the conservation of "mass" and "momentum" (more correctly, wave action flux). Another useful form is

$$U = \frac{3\eta}{2}\,, \quad U_\sigma + 6UU_\xi + h^{9/4}U_{\xi\xi\xi} \; = \; 0\,, \tag{5}$$

$$\sigma = \frac{1}{6}\int_0^\tau \frac{d\tau'}{h^{5/4}(\tau')} = \frac{1}{6}\int_0^x \frac{dx'}{h^{7/4}(x')}\,. \tag{6}$$

In this formulation we assume that $h = 1$ when the depth is constant, and then $h < 1$ when the wave moves up a slope.

On a constant depth the KdV equation (5) has the well-known soliton (solitary wave) solution

$$U = A\,\mathrm{sech}^2(K(\xi - V\sigma)) , \quad V = 2A = 4K^2 . \tag{7}$$

Here we are concerned with the "initial" value problem when $U = U_0(\xi)$ at $\sigma = 0$. Note that this is in fact a specification of a wave at an initial location, and the equation then describes the spatial evolution. It is well known that if $U_0(\xi) \geq 0$ (elevation), then several solitons are generated, but if instead $U_0(\xi) \leq 0$,(depression) then no solitons are generated, and instead the solution disperses with the front being described by a nonlinear Airy-type function. This has the shape of an initial depression, followed by a series of elevation waves riding on a negative pedestal, see El (2007), Segur (2007) and Arcasi and Segur (2012) for instance.

Consider, for example, the case when $U_0(\xi) = \pm G(\xi)$, respectively an initial wave of elevation, or depression, where $G(\xi) \geq 0$ is a localised pulse, for instance a Gaussian. Then in the elevation case, $N$ rank-ordered solitons are produced, with $N$ amplitudes, together with some trailing dispersing radiation. When $N$ is large, the soliton amplitudes are distributed according to the law

$$A \sim \frac{\xi}{2\sigma} , \quad 0 < \frac{\xi}{4\sigma} < G_M = 2 \max G(x) . \tag{8}$$

In particular the leading emerging solitary wave has an amplitude of $2G_M$, see El (2007).

In the depression case the long-time evolution can be modelled as a rarefaction wave (an exact solution of (5)) given by

$$\begin{aligned} &U = 0 , \quad \xi > 0 , \\ &U = \frac{\xi}{6\sigma} , \quad -L(\sigma) < \frac{\xi}{6\sigma} < 0 , \\ &U = 0 , \quad \frac{\xi}{6\sigma} < -L(\sigma) , \\ &\text{where} \quad 3\sigma L^2 = M = \int_{-\infty}^{\infty} |G(\xi)|\, d\xi . \end{aligned} \tag{9}$$

Here $L(\sigma)$ is determined by conservation of mass. This solution is an $N$-wave, and at $\xi = 6\sigma L$, there is jump $L$ from the negative level $-L$ to 0. This is resolved by an undular bore whose leading wave is a solitary wave of amplitude $2L$, relative to the pedestal of $-L$, see Grimshaw (2001) and El (2007) for instance. Thus the amplitude of this leading solitary wave is $2(M/3\sigma)^{1/2}$. This can be larger than the leading solitary wave from an elevation initial condition, when $\sigma < M/3G_M^2$. Note that here $M, G_M$ are independent parameters, and this estimate suggests that the leading elevation wave on a depression wave emanating from a depression initial condition will be greater than the leading elevation wave from an elevation initial condition when $M$ is large, but $G_M$ is small. The laboratory experiments of Hammack and Segur (1978) exhibit this behaviour, see figures 2 and 3 in the review by Arcasi and Segur (2012).

When there is a slope, there are no analogous asymptotic solutions available. However it is known that a single solitary wave will deform adiabaticaly as $h^{-1}$, see El *et al* (2012) and the references therein. However, the numerical study by El *et al* (2012) indicates that a KdV undular bore of elevation propagating up a slope develops a quite complicated structure, but the leading solitary wave does deform as $h^{-1}$. When the initial wave is one of depression, then the rarefaction wave of depression (9) again holds even when $h$ in equation (5) varies. Hence we would again expect an undular bore to develop at the trailing edge, with the leading solitary wave in the undular bore deforming adiabatically. Indeed, this behaviour was found in the experiments by Klettner *et al* (2012) describing of an initial depression up a slope, see their figure 5 especially.

# 3 Extended Korteweg-de Vries equation

## 3.1 Derivation

The extended Korteweg-de Vries equation (eKdV) for water waves on a constant depth is an extension of (1) when a cubic nonlinear term is included,

$$\zeta_t + c\zeta_x + \frac{3c}{2h}\zeta\zeta_x + \beta\zeta^2\zeta_x + \frac{ch^2}{6}\zeta_{xxx} = 0\,. \tag{10}$$

The coefficient $\beta$ can be found from the literature,see Marchant and Smyth (1990) for instance, or more directly by noting that in the absence of dispersion, the Riemann invariant solution from nonlinear shallow water theory is,

$$R_t + VR_x = 0\,, \quad R = U + 2C\,,\ V = U + C\,, \quad C = \sqrt{h+\zeta}\,, \quad L = U - 2C = -2\sqrt{h}\,. \tag{11}$$

Here $R, L$ are the right-going and left-going Riemann invariants, and the left-going wave has been set to the constant background. Hence,

$$\zeta_t + V\zeta_x = 0\,,\,, \quad V = 3\sqrt{h+\zeta} - 2\sqrt{h} = c + \frac{3c}{2h}\zeta - \frac{3c}{8h^2}\zeta^2 + \cdots\,. \tag{12}$$

Hence we infer that $\beta = -3c/8h^2$, which is the opposite sign to that needed for the eKdV equation to have breather solutions.

However, noting that the coefficient $\beta$ is not unique, here we adopt a different approach. First we note that (11) can be expressed in terms of $V$,

$$V_t + VV_x = 0\,. \tag{13}$$

Indeed, this is exact, and shows that in terms of the variable $V$, $\beta = 0$. More generally the Riemann invariant equation (12) can be written as

$$Z_t + VZ_x = 0 \quad Z = Z(\zeta)\,, \quad V = V(Z)\,, \tag{14}$$

where $Z(\zeta)$ can be chosen arbitrarily. Here we choose $Z$ so that

$$V(Z) = c + \frac{3c}{2h}Z + \frac{3c\beta}{2h^2}Z^2 \,. \tag{15}$$

Here $\beta > 0$ can be chosen arbitrarily. Then combining this with the expression for $V(\zeta)$ in (12) defines the function $Z(\zeta)$,

$$(1 + \frac{\zeta}{h})^{1/2} - 1 = \frac{Z}{2h} + \frac{\beta Z^2}{2h^2} \,, \quad \text{so that} \quad Z(\zeta) = \zeta - \frac{\zeta^2}{2h} + \cdots \,. \tag{16}$$

Thus in the limit when $\zeta \ll h$, we infer that (16) is a near-identity transformation as then $Z \approx \zeta$. In this limit an eKdV equation with a positive cubic coefficient is a viable model, albeit in terms of the augmented variable $Z$,

$$Z_t + c\zeta_x + \frac{3c}{2h}ZZ_x + \frac{3c\beta}{2h^2}Z^2Z_x + \frac{ch^2}{6}Z_{xxx} = 0 \,. \tag{17}$$

Although the dispersive term has been approximated by this small-amplitude limit, we can keep the fully nonlinear relationship between $Z$ and $\zeta$ in (16).

## 3.2 Solitons and breathers

First we put (17) into canonical form,

$$Z = \frac{h}{\beta}v \,, \quad x - ct = \frac{h}{6^{1/2}}X \,, \quad t = \frac{h}{c6^{1/2}}T \,, \tag{18}$$

$$v_T + 6vv_X + 6v^2v_X + v_{XXX} = 0 \,. \tag{19}$$

The soliton and breather solutions can be found in the following form, Slunyaev (2001) and Chow *et al* (2005),

$$v = 2\{\tan^{-1}(\frac{g}{f})\}_X = \frac{2}{f^2 + g^2}(fg_X - gf_X) \,, \tag{20}$$

where $f, g$ are expressed in terms of exponential functions, sometimes including algebraic terms.

The 1-soliton solution is given by

$$\begin{aligned} &g = 1 + sa\exp(\gamma Y) \,, \quad f = 1 + sb\exp(\gamma Y) \,, \\ &Y = X - \gamma^2 T \,, \quad a, b = \frac{1 \pm \gamma}{\sqrt{1 + \gamma^2}} \,, \quad s = \pm 1 \,, \\ &v = \frac{\gamma^2}{1 + s\sqrt{1 + \gamma^2}\cosh(\gamma Y)} \,. \end{aligned} \tag{21}$$

Here $s = \pm 1$ corresponds to an elevation wave of amplitude $A = \sqrt{\gamma^2 + 1} - 1$ and a depression wave of amplitude $A = -\sqrt{\gamma^2 + 1} - 1$ respectively. As $\gamma$ varies over the range

$0 < \gamma < \infty$ the elevation wave amplitude lies in the range $0 < A < \infty$, while the depression wave amplitude lies in the range $-2 > A > -\infty$. For the same speed, the depression wave has the larger amplitude magnitude, but for the same amplitude magnitude, the elevation wave is faster. In general, the elevation wave with index 1 is faster than the depression wave with index 2 when $\gamma_1 > \gamma_2$, but will have the smaller amplitude magnitude when $\sqrt{1+\gamma_1^2} - 1 < \sqrt{1+\gamma_2^2} + 1$, which is always the case when $\gamma_1^2 < 8$, and remains the case unless $\gamma_1^2$ is sufficiently large, and sufficiently greater than $\gamma_2^2$.

Now consider a 2-soliton solution with far-field parameters $\gamma_1, \gamma_2$, given by, adapted from (11) in Chow *et al* (2005),

$$\begin{aligned}
&g = 1 + s_1 a_1 \exp(\phi) + s_2 a_2 \exp(\psi) + s_1 s_2 a_{12} \exp(\phi + \psi)\,, \\
&f = 1 + s_1 b_1 \exp(\phi) + s_2 b_2 \exp(\psi) + s_1 s_2 b_{12} \exp(\phi + \psi)\,, \\
&\phi = \gamma_1 X - \gamma_1^3 T\,, \quad \psi = \gamma_2 X - \gamma_2^3 T\,, \quad a_n, b_n = \frac{1 \pm \gamma_n}{\sqrt{1+\gamma_n^2}}\,, \quad n = 1, 2\,, \\
&a_{12}, b_{12} = \frac{(\gamma_1 - \gamma_2)^2}{(\gamma_1 + \gamma_2)^2} \frac{[1 \pm (\gamma_1 + \gamma_2) - \gamma_1 \gamma_2]}{\sqrt{1+\gamma_1^2}\sqrt{1+\gamma_2^2}}\,.
\end{aligned} \tag{22}$$

Without loss of generality, take $\gamma_2 > \gamma_1$. In the far field as $T \to \pm\infty$ the soliton limits are found by either fixing the phase $\phi$ and letting $\psi \to \mp\infty$ for the index 1, or fixing the phase $\psi$ and letting $\phi \to \pm\infty$ for the index 2. The outcome is, for index 1,

$$\begin{aligned}
&g \sim 1 + s_1 a_1 \exp(\phi)\,, \quad f \sim 1 + s_1 b_1 \exp(\phi)\,, \quad T \to \infty\,, \\
&g \sim a_2 + s_1 a_{12} \exp(\phi)\,, \quad f \sim b_2 + s_1 b_{12} \exp(\phi)\,, \quad T \to -\infty\,,
\end{aligned} \tag{23}$$

and for index 2,

$$\begin{aligned}
&g \sim a_1 + s_2 a_{12} \exp(\psi)\,, \quad f \sim b_1 + s_2 b_{12} \exp(\psi)\,, \quad T \to \infty\,, \\
&g \sim 1 + s_2 a_2 \exp(\psi)\,, \quad f \sim 1 + s_2 b_2 \exp(\psi)\,, \quad T \to -\infty\,.
\end{aligned} \tag{24}$$

Note that common factors in $f, g$ can be removed. Each of these are easily recognised as the corresponding 1-soliton solutions, but with a phase shift from $T \to -\infty$ to $T \to \infty$, given by

$$\exp(-\Delta\phi), \exp(\Delta\psi) = \frac{(\gamma_2 + \gamma_1)^2}{(\gamma_2 - \gamma_1)^2}\,. \tag{25}$$

This agrees with the expression (11) in Slunyaev (2001). Note that $\Delta\phi < 0, \Delta\psi > 0$, so the faster wave is shifted forwards and the slower wave is shfted backwards.

Our interest here is in the case when the depression wave precedes the elevation wave as $T \to -\infty$, so that the depression and elevation wave have indices $1, 2$ respectively, that is $s_1 = -1, s_2 = 1$. Then the elevation wave will catch up with the depression wave, and there will be an interaction at the approximate location $X = 0, T = 0$. Taking account of the phase shifts (25) this can be refined to $X = X_{int}, T = T_{int}$ where

$$(\gamma_2^2 - \gamma_1^2) X_{int} = -\frac{\gamma_1^2 \Delta\phi}{2\gamma_1} - \frac{\gamma_1^2 \Delta\psi}{2\gamma_2}\,, \quad (\gamma_2^2 - \gamma_1^2) T_{int} = -\frac{\Delta\phi}{2\gamma_1} - \frac{\Delta\psi}{2\gamma_2}\,. \tag{26}$$

Slunyaev (2001) (see equation (10)) provides an estimate that at the interaction centre the amplitude is $A_2 - A_1$, where $A_1 < 0, A_2 > 0$ are the far-field amplitudes. The interaction is like that of a breather, and at the centre there is enhanced elevation, lying between $2\min[A_1, A_2]$ and $2\max[A_1, A_2]$. This is twice the far-field value when $|A_1| = A_2$. A set of typical results are shown in figures 1 and 2 for the cases when $\gamma_1 = 0.7, \gamma_2 = 3.0$ and $\gamma_1 = 1.3, \gamma_2 = 3.4$ respectively. These represent two solitons of nearly equal amplitudes, $A_1 = -2.22, A_2 = 2.16$ and $A_1 = -2.64, A_2 = 2.54$ respectively, so that the depression wave is slightly larger in magnitude, but considerably slower in speed. Then in figures 3 and 4 we plot the cases when $\gamma_1 = 0.7, \gamma_2 = 0.72$ and $\gamma_1 = 1.3, \gamma_2 = 1.5$ so that now the speeds are quite close, but the elevation wave is faster, while the amplitudes are quite different with a much larger depression wave, $A_1 = -2.22, A_2 = 0.23$ and $A_1 = -2.64, A_2 = 0.8$ respectively. These cases are similar to figures 3 and 4 of Slunyaev (2001), but there the speeds were much faster.

The breather solution can be found by formally putting $\gamma_{1,2} = m \pm in$, $m, n > 0$ in (22), see (14) in Slunyaev (2001), or (13) in Chow *et al* (2005). The outcome is, obtained by setting here by setting $s_1 = s_2 = 1$ and adjusting the phases appropriately,

$$\begin{aligned}
g &= 1 - \frac{n^2}{m^2}\frac{1+2m-(m^2+n^2)}{1-2m+(m^2+n^2)}\exp(2m\theta) + 2(\xi\cos(n\Theta) - \eta\sin(n\Theta))\exp(m\theta)\,,\\
f &= 1 - \frac{n^2}{m^2}\frac{1-2m-(m^2+n^2)}{1-2m+(m^2+n^2)}\exp(2m\theta) + 2\cos(n\Theta)\exp(m\theta)\,,\\
\theta &= X - (m^2-3n^2)T\,, \quad \Theta = X - (3m^2-n^2)T\,,\\
\xi &= \frac{1-(m^2+n^2)}{1-2m+m^2+n^2}\,, \quad \eta = \frac{2n}{1-2m+m^2+n^2}\,.
\end{aligned} \tag{27}$$

The breather has two phases, $\theta$ and $\Theta$. It is localised in the phase $\theta$ and propagates with a speed $C = m^2 - 3n^2$, and oscillates in the phase $\Theta$ with a frequency $n\Omega\,, \Omega = 3m^2 - n^2$. In the reference frame moving with speed $C$, set $Y = X - CT$ and then $\Theta = n(Y - 2(m^2+n^2))T$. Hence in this frame it has a period

$$P = \pi/n(m^2+n^2)\,. \tag{28}$$

In the limit $n \gg m$ there are many crests inside the envelope and it resembles an envelope wave packet. In the opposite limit when $n \ll m$, it resembles a two soliton interaction, see Figure 5 of Slunyaev (2001) or Figure 4 of Chow *et al* (2005). This is the case of interest here, and describes the interaction of two solitons of opposite polarity and almost equal speeds. Hence the depression soliton has the larger amplitude. The greatest distance apart is

$$L = \frac{2}{m}\log\frac{2m}{n}\,. \tag{29}$$

The double pole solution can be found by again choosing special phases and taking the limit $n \to 0$ in (27), see Chow *et al* (2005),

$$
\begin{aligned}
g &= 1 - \frac{1+2m-m^2}{m^2(1-m)^2}\exp(2m\theta) + \frac{2[(1-m^2)\Theta+2]\exp(m\theta)}{(1-m)^2}\,, \\
f &= 1 - \frac{1-2m-m^2}{m^2(1-m)^2}\exp(2m\theta) + 2\Theta\exp(m\theta)\,, \\
\theta &= X - m^2 T\,, \quad \Theta = X - 3m^2 T = \theta - 2m^2 T\,.
\end{aligned}
\tag{30}
$$

A typical result is shown in Figure 4 of Chow *et al* (2005). In the far field as $T \to -\infty$ this is an elevation wave chasing a larger amplitude depression wave. They coincide around $T = 0$, and then as $T \to \infty$ the elevation wave goes ahead. In detail, for fixed phase $\theta$, as $T \to \pm\infty$, the solution collapses to two single waves, each approximately a single wave, propagating with speed $V \sim m^2$, and hence with expected amplitudes $\sim \pm\sqrt{1+m^2} - 1$, see (21). Each wave phase can be described asymptotically for large $|T|$ by,

$$
m\theta \sim \pm\mathrm{sign}\{T\}\log(Km^2|T|)\,, \quad \text{so that} \quad V \sim m^2 \pm \frac{1}{m|T|}\,,
\tag{31}
$$

where the alternate signs refer to the faster/slower wave respectively. $K$ is a positive constant to be determined and depends both on which wave is being considered, and on which limit, that is either $T \pm \infty$. The speeds become equal in the long time limit, and the two waves separate as $\log|T|$. From (30), we can write $v = 2N/D$, $D = f^2 + g^2 > 0$, and

$$
\begin{aligned}
N &= fg_X - gf_X = \Theta[\alpha_3\exp(3m\theta) + \alpha_1\exp(m\theta)] + \\
&\quad [\beta_3\exp(3m\theta) + \beta_2\exp(2m\theta) + \beta_1\exp(m\theta)]\,, \\
\alpha_3 &= -\frac{4(1+m^2)}{(1-m)^3}\,, \quad \alpha_1 = \frac{4m^2}{(1-m)}\,.
\end{aligned}
\tag{32}
$$

Note that $\alpha_3 < 0, \alpha_1 > 0$ when $0 < m < 1$, and $\alpha_3 > 0, \alpha_1 < 0$ when $m > 1$. These expressions can be evaluated on the trajectories (31), where we note that then $\Theta \sim -m^2 T$ with a logarithmic error. As $T \to -\infty$, $\exp(m\theta) \sim (Km^2|T|)^{\mp 1}$, and as $T \to \infty$, $\exp(m\theta) \sim (Km^2|T|)^{\pm 1}$, for the faster and slower waves respectively. It then follows that, for the faster wave,

$$
\begin{aligned}
&N \sim \frac{\alpha_1}{K}\,,\ D \sim (1 + \frac{2}{K})^2 + (1 + \frac{2a_1}{K})^2\,,\ \alpha_1 = \frac{1+m}{1-m}\,,\ T \to -\infty\,, \\
&N \sim -m^8K^3\alpha_3T^4, D \sim m^8K^2T^4\{(f_1K+2)^2 + (g_1K + 2\alpha_1)^2\}\,,\ T \to \infty\,.
\end{aligned}
\tag{33}
$$

Here $f_1, g_1$ are the coefficients of the term $\exp(2m\theta)$ in the expressions (30) for $f, g$ respectively. In both limits, the amplitude is a constant as required, and is positive for $0 < m < 1$ and negative for $m > 1$. For the slower wave,

$$
\begin{aligned}
&N \sim m^8K^3\alpha_3T^4, D \sim m^8K^2T^4\{(f_1K-2)^2 + (g_1K - 2\alpha_1)^2\}\,,\ T \to \infty\,. \\
&N \sim -\frac{\alpha_1}{K}\,,\ D \sim (1 - \frac{2}{K})^2 + (1 - \frac{2a_1}{K})^2\,,\ \alpha_1 = \frac{1+m}{1-m}\,,\ T \to -\infty\,,
\end{aligned}
\tag{34}
$$

Again, in both limits, the amplitude is a constant as required, and is now negative for $0 < m < 1$ and positive for $m > 1$. Note that only the leading order term in $N$ is needed here in all cases, and the term in $[\cdots]$ is not needed. Also we see that $|2N/D|$ depends on $K$ and in all cases is zero as $K \to 0, \infty$ and has a maximum value when

$$K = \frac{2(1+m^2)^{1/2}}{|1-m|}\,,\ \text{Cases}\, f_-, s_+\,;\ K = \frac{2m^2|1-m|}{(1+m^2)^{1/2}}\,,\ \text{Cases}\, f_+, s_-\,. \tag{35}$$

Here the notation $f_{\pm}, s_{\pm}$ denote the faster or slower wave as $T \to \pm\infty$ respectively. Then evaluation of the corresponding amplitudes $2N/D$ at these values of $K$ are indeed $\pm\sqrt{1+m^2} - 1$ according as the wave is one of elevation or depression, as expected. Using these expressions we can deduce from (31) that the faster and slower wave have phase shifts from $T \to \infty$ to $T \to \infty$ of $\pm\Delta\theta$ where

$$\Delta\theta = \log\{\frac{1+m^2}{m^2(1-m)^2}\}\,. \tag{36}$$

Finally, we can deduce from the phase expressions (31) that if the two waves are located a distance $2X_0$ apart at a time $\pm T_0$ as $T \to \pm\infty$, then

$$X_0 \approx \log(2m^2 T_0)\,. \tag{37}$$

Plots of (30) for $m = 0.7, 1.3$ are shown in figures 5 and 6 respectively. Note that figure 5 is similar to figure 4 of Chow *et al* (2005), and also to the 2-soliton solution shown in figures 3 and 4 above, although note that as discussed above, the time scale of approach and separation are quite different for this breather case. The amplitudes at $t = \pm 50$ are in good agreement with the theoretical predictions as $t \to \pm\infty$ indicating that the asymptotic state has been reached. In figure 5 where $0 < m < 1$ the faster wave is one of elevation and the slower wave is one of depression. At the time of interaction, which is close to $T = 0$ and can be estimated from the phase shifts (36) we see that these waves combine into a large elevation whose height is approximately given by the absolute sum of the amplitudes at infinity, that is given here by $2\sqrt{1+m^2}$. This scenario is reversed in figure 6 where $m > 1$ as now the faster wave is one of depression and the slower wave is one of elevation, with the consequence that at the time of interaction the waves combine into a large depression whose amplitude is approximately $-2\sqrt{1+m^2}$.

# 4 Discussion and applications

In this paper we have used the traditional KdV model (section 2) and a new eKdV model (section 3) to examine the dynamics of a down-up wave, that is a depression wave followed by an elevation wave. This approach differs from the extensive literature on $N$-waves found using the usual non-dispersive nonlinear shallow water equations, in that these models importantly include the effects of weak linear wave dispersion. We note that Arcasi and Segur (2012) recently called attention to the necessity to invoke wave dispersion when describing tsunami waves of depression. The KdV model, whether for a constant depth, or on a slope, indicates that a initial depression develops into a depression wave followed by a series of elevation waves riding on this negative pedestal, see Arcasi and Segur (2012) for instance. and the leading wave may have an amplitude magnitude twice that of the leading depression. We have already noted that this scenario is qualitatively similar to that seen in the wave tank experiments of Klettner *et al* (2012) where an initial wave of depression travelled up a slope. When the expressions in equation (9) and the following text are translated to the original dimensional variables through the transformations in equations (3) - (6), we find that the predicted height of the leading solitary wave is $2L_d$, $L_d = 2(4M_d h/3x_d)^{1/2}$, riding relative to a pedestal of $-L_d$ where $M_d$ is the initial total displaced volume, and $x_d$ is the distance travelled. From figure 5(a) of Klettner *et al* (2012) we estimate that $M_d = 0.03\,m^2$ and then when $x_d = 20.68\,m$ we find that $L_d = 0.04\,m$, in quite good agreement with the observed value of about $0.05\,m$. Note that here we have not taken account of the wave amplification over the slope,and this would account for the underestimate. Indeed at the location $x_d$ the depth in the wave tank has decreased from $0.8\,m$ to $0.7\,m$ and assuming the adiabatic expression of $h^{-1}$ for a solitary wave, this would increase our estimate of $L_d$ to $L_d = 0.046\,m$.

However, in these KdV models this combination of a depression and elevation waves is an unsteady wave train, and so the complete structure eventually fully disperses. Hence in a search for models supporting more persistent structures, we have invoked a higher-order model, the eKdV equation (17). Although this eKdV model supports interacting depression and elevation waves through families of two-soliton and breather solutions, we must note two issues concerning the application of this model to water waves. First, we note that the balance of terms in (17) is such that the nonlinear terms have a larger magnitude than the linear dispersive term. If a small-amplitude hypothesis is invoked to remedy this, then the outcome is that the cubic nonlinear term is suppressed *vis-a-vis* the quadratic nonlinear term. This then eliminates the depression soliton, the two-soliton solution, when comprising both elevation and depression waves, and the breather solution of interest here, as all these require a balance between the quadratic and cubic nonlinear terms. Second, although one might accept that (17) can be used in the *ad hoc* sense that the role of the linear dispersive term is to provide a weak dispersive regularisation of the fully nonlinear equation (14) which is valid within the fully nonlinear shallow water framework, the application to water waves requires use of the relationship $Z(\zeta)$ expressed in (16) and then again $Z \approx \zeta$ only when $\zeta \ll h$. Nevertheless, we maintain that these solutions in particular have qualitative features which resemble laboratory and field observations of some tsunami waves, and suggest that this eKdV model may have some value when properly interpreted. In particular we focus on the interaction scenarios displayed in the middle panel of figures 1 to 5 as here the solutions are predominately positive and then we can invoke the relationship $Z(\zeta)$ in (16) in the limit when $Z \approx \zeta$ to obtain a physical interpretation.

The expressions presented in section 3.2 provide a complete explicit description of the interaction of a depression and elevation wave, and from these we can extract the essential information on the timescale for the interaction, and the wave amplitude at the centre of the interaction. There are two main kinds of two-soliton interaction; one in which the depression and elevation components have similar amplitudes, shown in figures

1, 2 and the other in which the two components have similar speeds, shown in figures 3, 4. The double-pole breather solution, shown in figures 5, 6, is essentially a limit of the two-soliton interaction when the speeds are identical. From the analytical expressions we can estimate a dimensional transition time, taking account of the scaling (18) and for simplicity assuming also that we can replace $Z$ with $\zeta$. Thus suppose that initially an elevation wave of amplitude $\Delta h_2$ is located at $x = -L_0$ behind a depression wave of amplitude $-\Delta h_1$ located at $x = +L_0$. The speed of each wave can be estimated from (12) as $c(1 \pm \Delta h_{1,2}/2h)$. From the two-soliton model, hese two approach each other linearly in time, and interact at a time and place given by

$$t^* \approx \frac{4hL_0}{c\zeta_{int}}\,, \quad x^* \approx \frac{4hL_0}{\zeta_{int}}\,, \quad \text{where} \quad \zeta_{int} = \Delta h_2 + \Delta h_1\,. \tag{38}$$

Here we also assumed that $\Delta h_{1,2} \ll h$, and $\zeta_{int}$ is the estimated elevation at the interaction site. On the other hand, from the double-pole breather model, the approach is logarithmic in time and the corresponding expressions for $t^*, x^*$ can be deduced from (37). However, then the interaction time and place are increased exponentially due to the slower logarithmic approach, and we find that these alternative expressions are not as applicable as (38). For instance, based on the available data recorded near Phuket Island for the Sumatra 2004 tsunami, see Ioulalen *et al* (2007) and Grilli *et al* (2007), we choose $\Delta h_2 = 3, \Delta h_1 = 3\,m$, $h = 25m$, $L_0 = 8\,km$, and then $t^* = 142\,min$, $x^* = 133\,km$ and $\zeta_{int} = 6\,m$. These estimates indicate that the peak interaction is close to the shoreline, although the bottom slope has not been taken into account, which would slow the wave interaction down and so reduce $x^*$. A similar scenario can be deduced from tide gauge data north of Sendai for the Tohoku 2011 tsunami, see Fujii *et al* (2011), Shimozono *et al* (2012) and Klettner *et al* (2012). Here we choose $\Delta h_2 = 4\,m, \Delta h_1 = 4\,m$, $h = 50\,m$, $L_0 = 16\,km$ as representative values, and then $t^* = 301\,min$, $x^* = 200\,km$ and $\zeta_{int} = 8\,m$. In this case these estimates indicate that the tsunami would reach the shore before the peak interaction occurs.

In conclusion, we suggest that the scenarios we have described here, both for the KdV and the eKdV models, are useful for understanding and possibly predicting the behaviour of down-up tsunami waves. In particular, as the plots we have shown demonstrate, there is a potential that the nonlinear interaction between the depression and elevation components can produce a striking elevation at the location of the interaction. It is to be emphasised that this outcome is more devastating than that caused by an incident elevation wave alone of the same initial height.

**Acknowledgement**: Hester H.N. Chan of the University of Hong Kong, and Kenyon K. Chow of the University of California at Los Angeles, assisted in the preparation of the figures.

# References

Arcasi, D. and Segur, H. (2012) Seismically generated tsunamis. *Phil. Trans. Royal Soc.*, **370**, 1505-1542.

Carrier G.F, Wu T.T. and Yeh H. (2003) Tsunami run-up and drawdown on a plane beach. *J. Fluid Mech.*, **475**, 79-99.

Charvet, I., Eames, I. and Rossetto, T. (2013) New tsunami run-up relationships based on long wave experiments. *Ocean Modelling*, **69**, 79-92.

Chow, K. W., Grimshaw, R. and Ding, E. (2005) Interactions of breathers and solitons in the extended Kortewegde Vries equation. *Wave Motion*, **43**, 158-166.

Dias, F. Dutykh, D., OBrien, L., Renzi, E. and Stefanakis, T. (2014) On the modelling of tsunami generation and tsunami inundation. *Procedia IUTAM*, **10**, 338-355.

Didenkulova I. and Efim Pelinovsky, E. (2011) Nonlinear wave evolution and run-up in an inclined channel of a parabolic cross-section.*Phys. Fluids*, **23**, 086602.

El, G. (2007) Kortweg-de Vries equation and undular bores. *In "Solitary waves in fluids", ed. R. Grimshaw, Advances in Fluid Mechanics, WIT Press*, **47**, 19-53.

El, G. A., Grimshaw R. H. J. and Tiong, W. K. (2012) Transformation of a shoaling undular bore, *J. Fluid Mech.*, **709**, 371-395.

Fernando H.J.S, Braun A, Galappatti R, Ruwanpura J and Wirisinghe S. C. (2008) Tsunamis: manifestation and Aftermath. In *Large Scale Disasters*. Cambridge University Press, Cambridge, UK, pp. 258-292.

Fujii, Y., Sakai, S., Shinohara, M. and Kanazawa, T. (2011) Tsunami source of the 2011 off the Pacific coast of Tohoku earthquake. *Earth Planets. Space*, **63**, 815-820.

Grilli, S.T., Ioualalen, M., Asavanant, J., Shi, F., Kirby, J.T and Watts, P. (2007) Source constraints and model simulation of the December 26, 2004, Indian Ocean tsunami. *J. Waterway Port Coastal and Ocean Engineering*, **133**, 414-428.

Grimshaw, R. (1981) Evolution equations for long nonlinear internal waves in stratified shear flows. *Stud. Appl. Math.* , **65**, 159-188.

Grimshaw, R. (2001). Internal solitary waves. *In "Environmental Stratified Flows", ed. R. Grimshaw, Kluwer*, 1-27.

Hammack, J. L. and Segur, H. (1978) The Kortewegde Vries equation and water waves. III. Oscillatory waves. *J. Fluid Mech.*, **84**, 337-358.

Ioualalen, M., Asavanant, J., Kaewbanjak, N., Grilli, S. T., Kirby, J. T. and Watts, P. Modeling the 26 December 2004 Indian Ocean tsunami: Case study of impact in Thailand *J. Geophys. Res.*, **112**, C07024.

Johnson, R. S. (1973a) On an asymptotic solution of the Korteweg - de Vries equation with slowly varying coefficients. *J. Fluid Mech.*, **60**, 813824.

Johnson, R. S. (1973b) On the development of a solitary wave moving over an uneven bottom. *Proc. Camb. Phil. Soc.*, **73**, 183203.

Klettner, C., Balasubramanian, S., Hunt, J., Fernando, H. Voropayaev, S. and Eames, I. (2012) Draw-down and run-up of tsunami waves on sloping beaches. *Eng. & Comp. Mech.*. **165**, 119-129.

Kobayashi N. and Lawrence A. R. (2004) Cross- shore sediment transport under breaking solitary waves. *J. Geophys. Res.*, **109**, C03047.

Kundu, A. Tsunamis and nonlinear waves (2007). *ed. A. Kundu, Springer*, 315 pp. b

Madsen, P.A. and Schaffer, H.A. (2010) Analytical solutions for tsunami run-up on a plane beach: single waves, N-waves and transient waves. *J. Fluid Mech.*, **645**, 27-57.

Marchant, T. R. and Smyth, N. F. (1990) The extended Korteweg-de Vries equation and the resonant flow of a fluid over topography. *J. Fluid Mech.*, **221**, 263-288.

Mori,N., Takahashi, T., Yasuda, T. and Yanagisawa, H. Survey of 2011 Tohoku earthquake tsunami inundation and run-up (2013) *Geophy. Res. Lett.*, **38** L00G14.

Rossetto, T., Allsop, W., Charvet, I. and Robinson, D. I. (2011) Physical modelling of tsunami using a new pneumatic wave generator. *Coastal Engineering*, **58**, 517-527.

Segur, H. Waves in shallow water, with emphasis on the tsunami of 2004 (2007). *In "Tsunamis and nonlinear waves", ed. A.Kundu*, Springer, 1-30.

Shimozono, T., Sato, T., Okayasu, A., Tajima, Y., Fritz, H. M, Liu, H. and Takagawa, T. (2012) Propogation and inundation characteristics of the 2011 Tohoku tsunami on the central Sanriku coast. *Coastal Engineering J.*, **54**, 125004.

Soloviev, S.L. and Mazova, R.K. (1994) On the influence of sign of leading tsunami wave on run-up height on the coast. *Science of Tsunami Hazards*, **12**, 2531.

Slunyaev, A. V. (2001) Dynamics of localized waves with large wmplitude in a weakly dispersive medium with a quadratic and positive cubic nonlinearity. *J. Exp. Th. Phys.*, **92**, 529-534.

Tadepalli, S. and Synolakis, C.E. (1994) The run-up of N-waves on sloping beaches. *Proc. Royal Soc. A*, **445**, 99-112.

Tadepalli, S. and Synolakis, C.E. (1996) Model for the leading wave of tsunamis. *Phys. Rev. Letters*, **77**, 2141-2144.

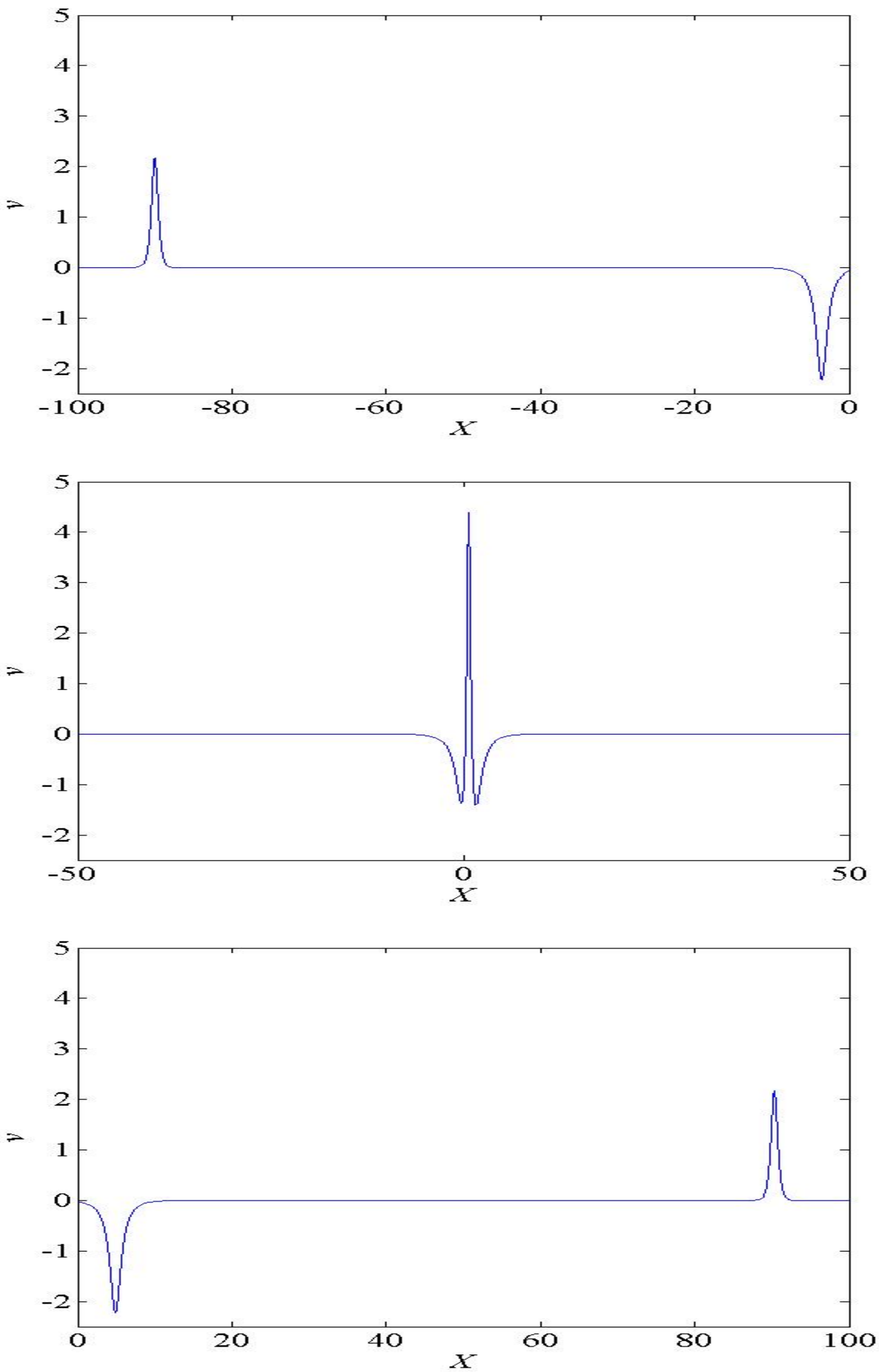


Figure 1: Plot of (22) for $\gamma_1 = 0.7, \gamma_2 = 3.0.$ at $t = -10, 0.06, 10$ from top to bottom.

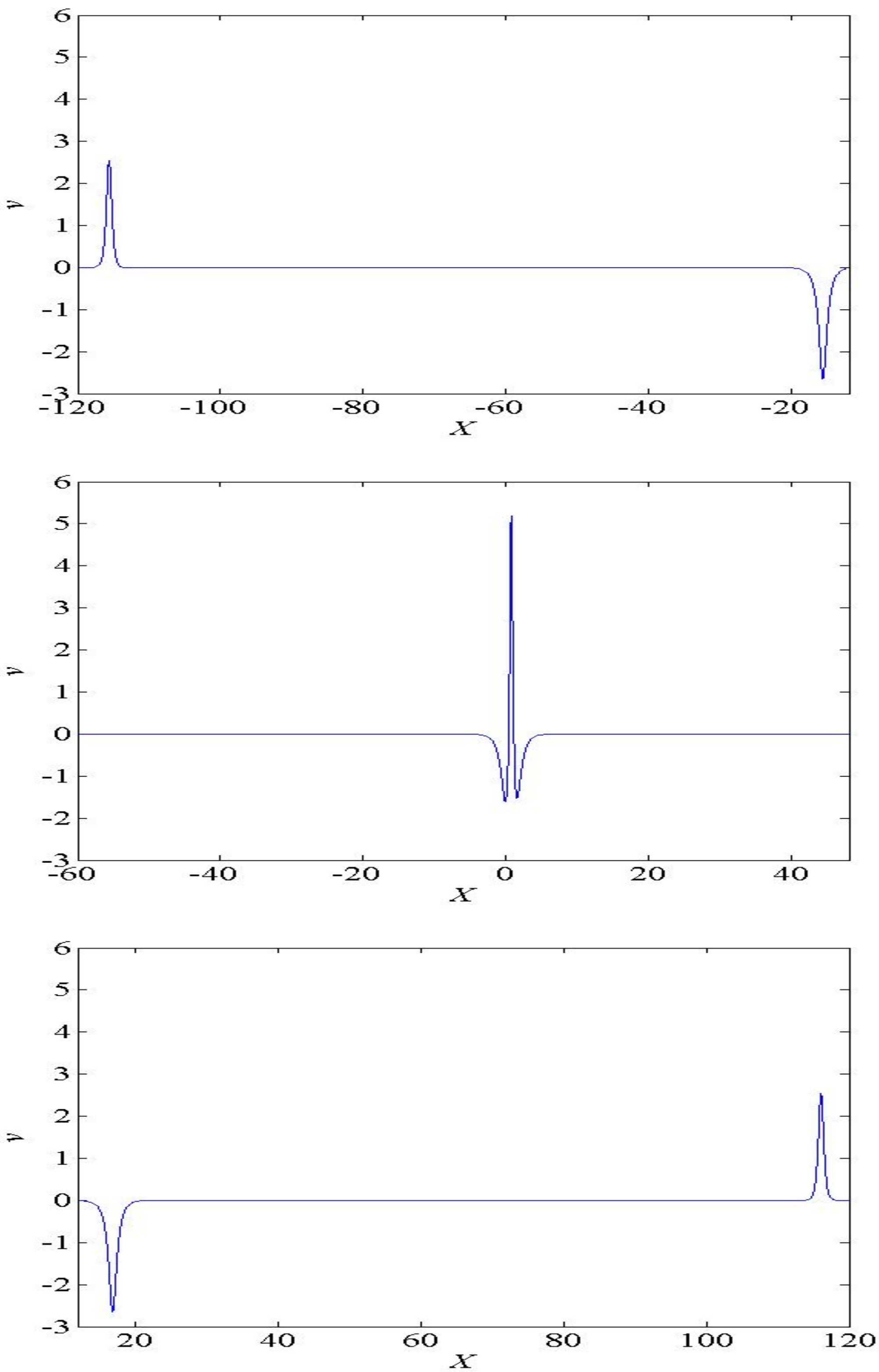


Figure 2: Plot of (22) for $\gamma_1 = 1.3, \gamma_2 = 3.4$ at $t = -10, 0.04, 10$ from top to bottom.

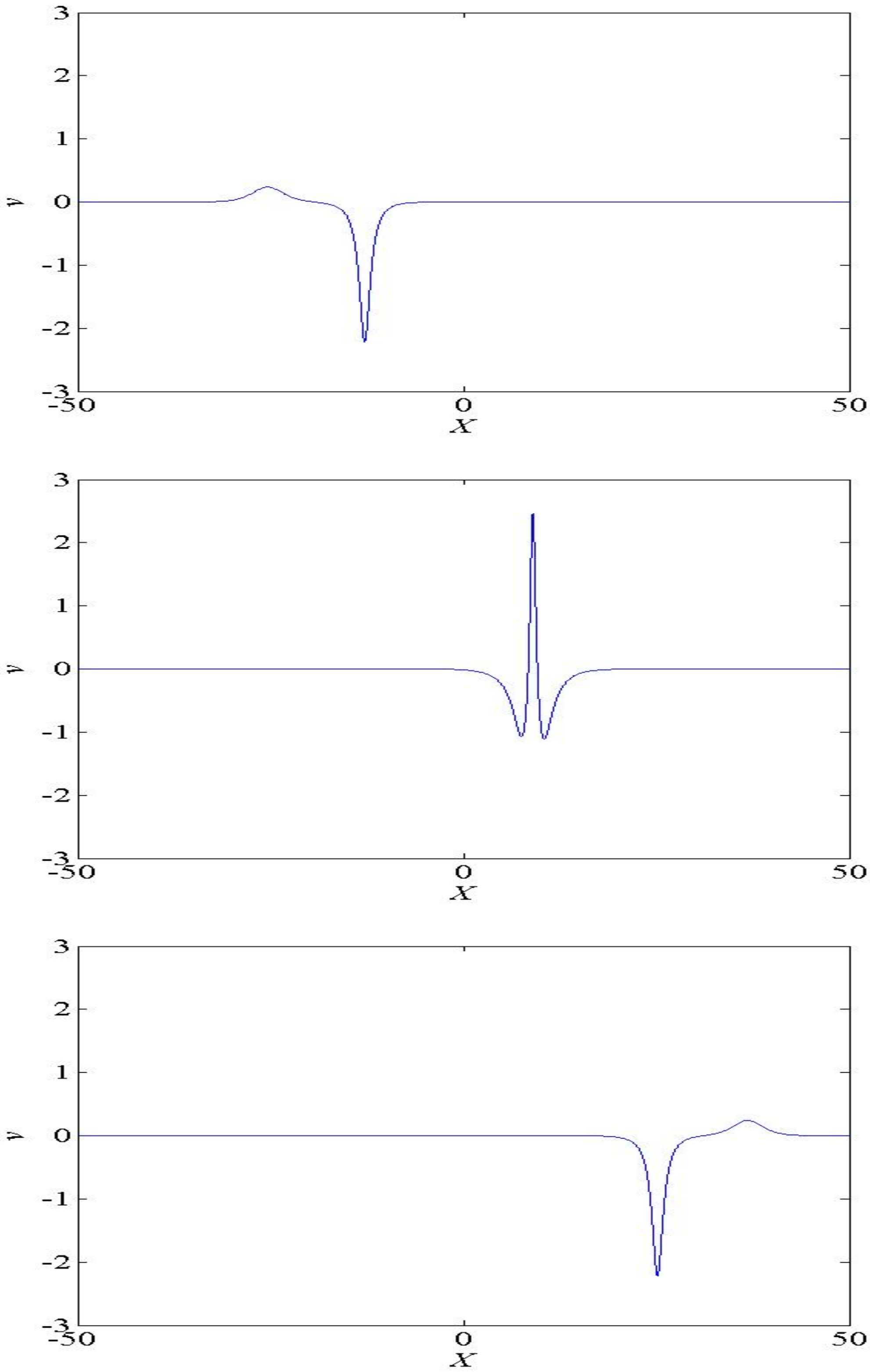


Figure 3: Plot of (22) for $\gamma_1 = 0.7, \gamma_2 = 0.72$. at $t = -50, 5.95, 50$ from top to bottom.

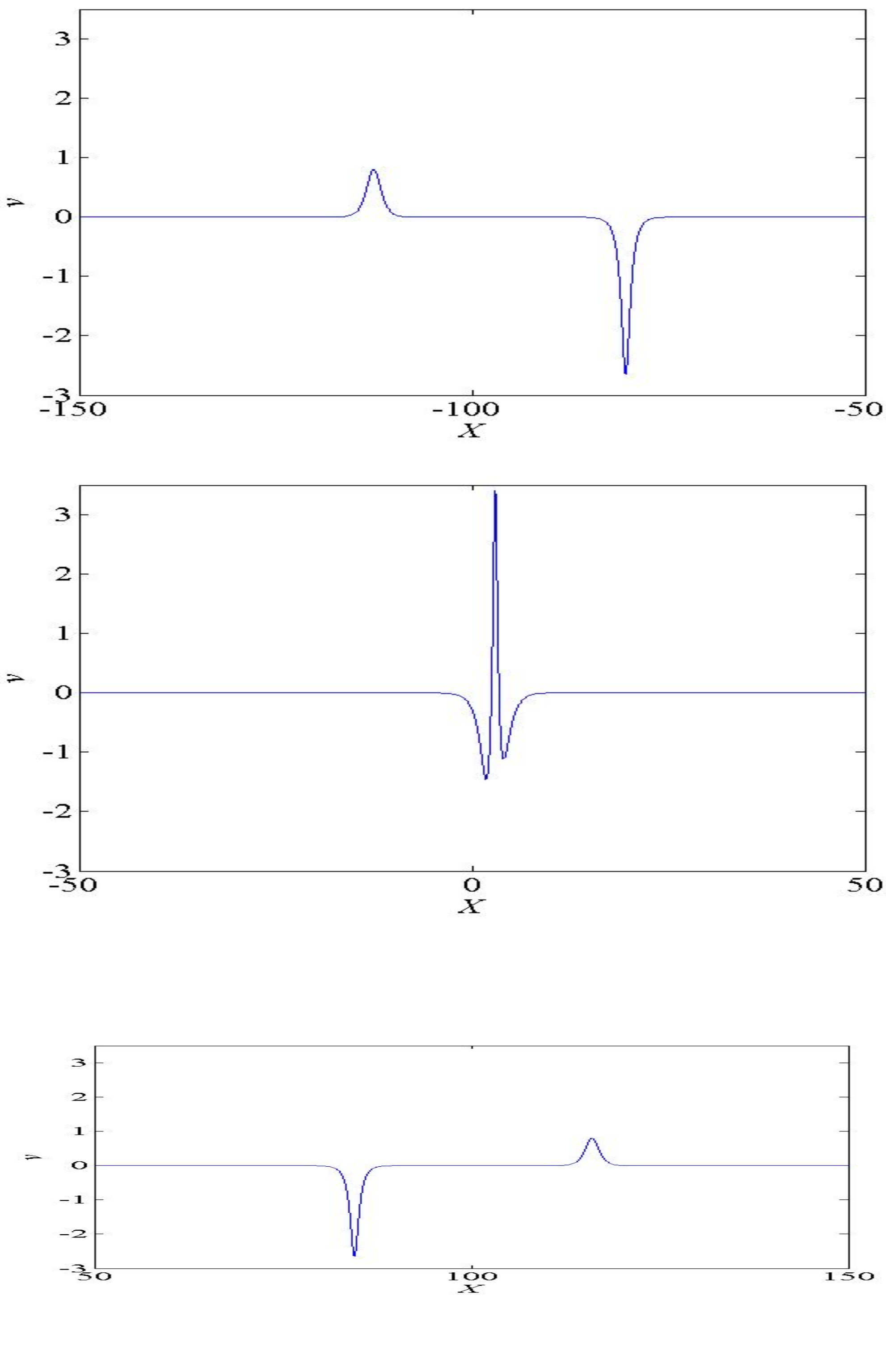


Figure 4: Plot of (22) for $\gamma_1 = 1.3, \gamma_2 = 1.5.$ at $t = -50, 0.5, 50$ from top to bottom.

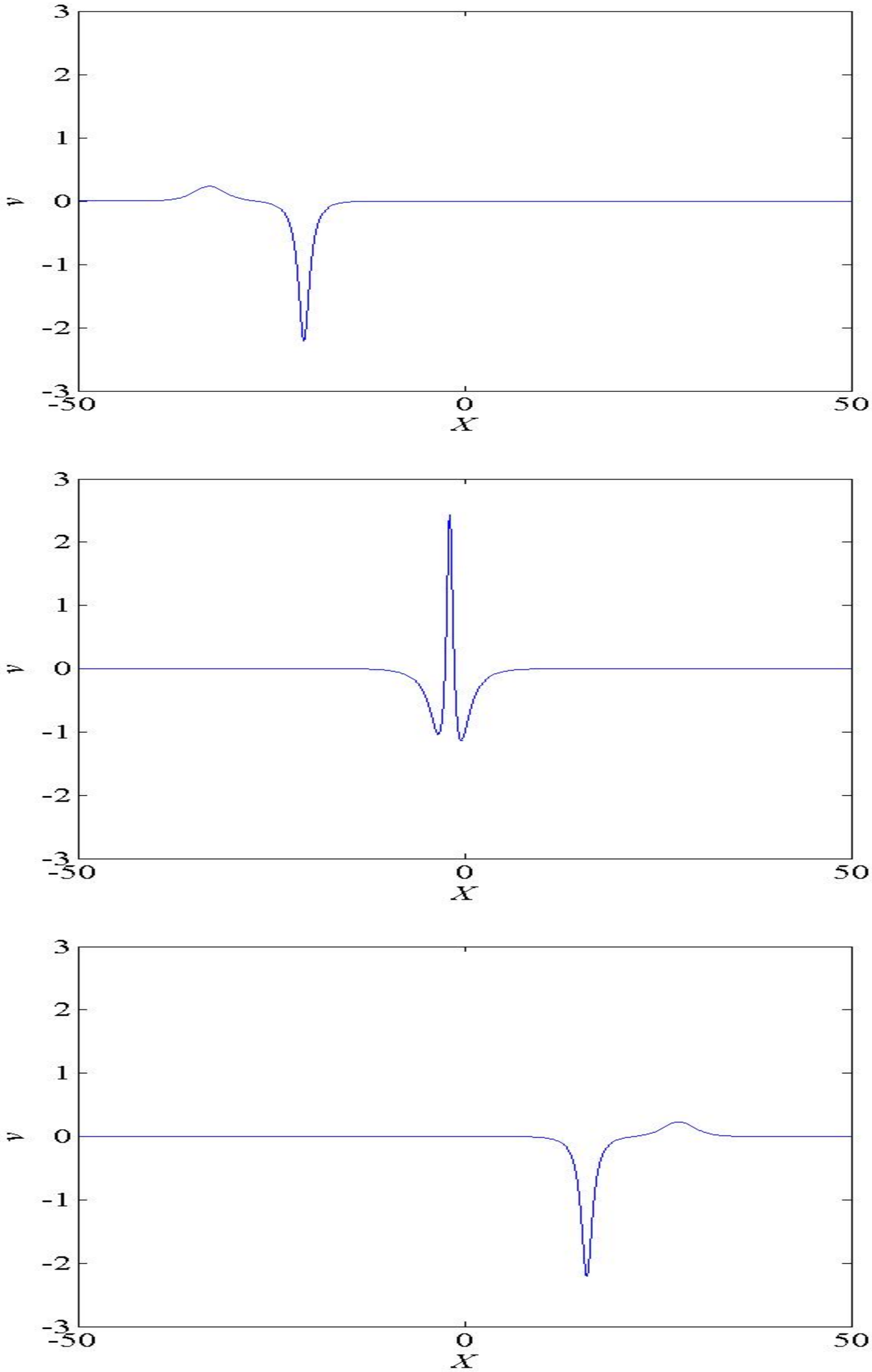


Figure 5: Plot of (30) for $m = 0.7$. at $t = -50, 1.3, 50$ from top to bottom.

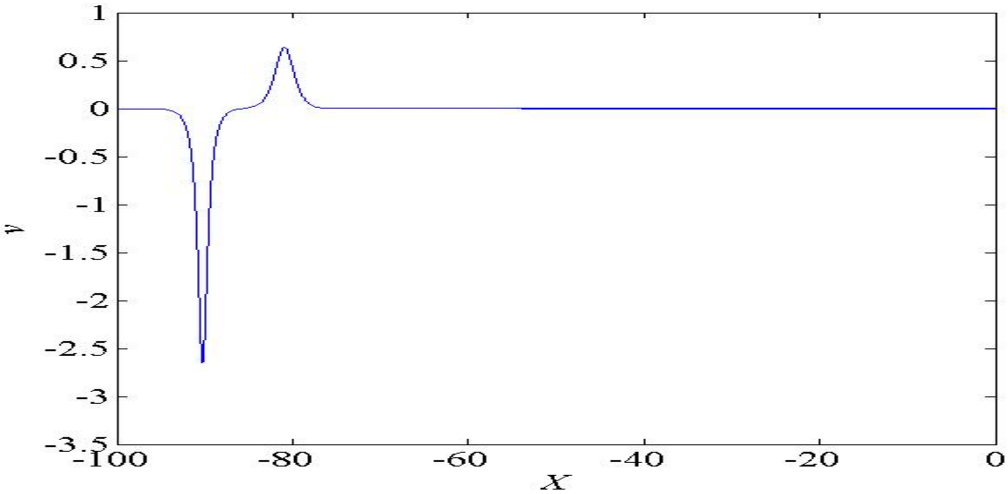


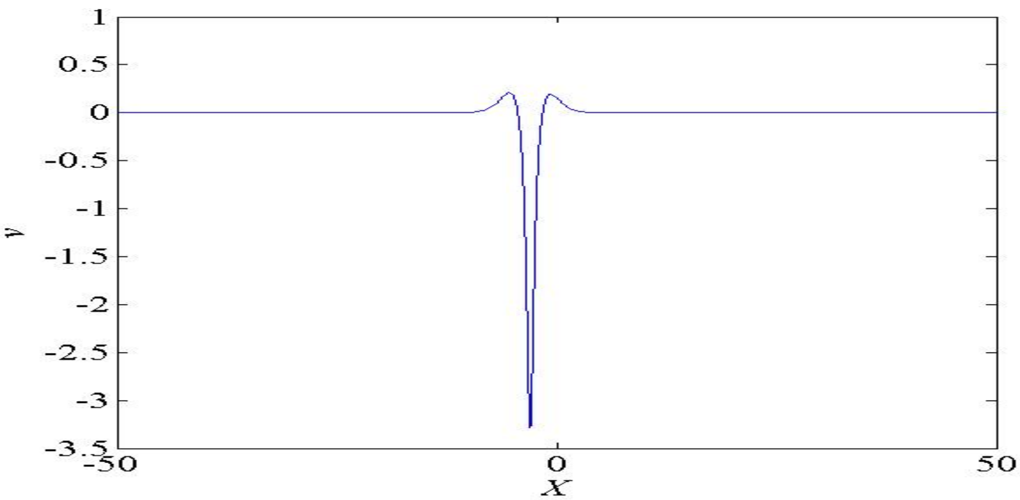


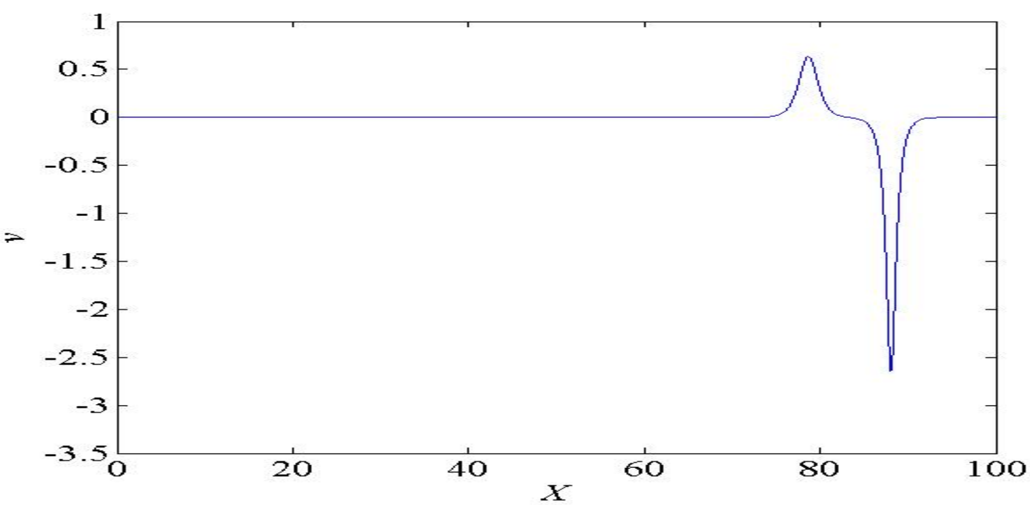


Figure 6: Plot of (30) for $m = 1.3$ at $t = -50, -1.15, 50$ from top to bottom.